Progress In Electromagnetics Research, PIER 78, 129–157, 2008

ULTRA WIDE BAND RCS OPTIMIZATION OF MULTILAYERED CYLINDRICAL STRUCTURES FOR ARBITRARILY POLARIZED INCIDENT PLANE WAVES

H. Oraizi and A. Abdolali

Department of Electrical Engineering,
Iran University of Science and Technology
Narmak, Tehran, 1684613114 Iran

Abstract—The addition theorems are applied to analyze the normal incidence of plane waves onto infinitely long conducting or dielectric circular cylinders with multilayer coatings made of common and uncommon materials $(\varepsilon_r, \mu_r, \sigma)$ with the objective of minimization and maximization of radar cross-section (RCS). TE, TM and circular polarizations of the incident wave are considered. Optimization of RCS by the method of least squares leads to the determination of layer thicknesses and the material complex permittivities and permeabilities. A sensitivity analysis of RCS with respect to the geometrical and material parameters of the multilayer coated conducting cylinder is also performed. It is observed that broadband reduction of RCS is mostly achievable by a combination of conventional materials $(\varepsilon_r,\ \mu_r > 1)$, and unconventional materials $(0 < \varepsilon_r,\ \mu_r < 1)$ and lossy materials $(\sigma > 0)$. It is seen that RCS reduction is due to the diversion and dissipation of radar signals. The results agree very well with the experimental and theoretical data available in the literature.

1. INTRODUCTION

Radar systems have wide civilian and military applications, such as remote sensing, meteorology, medicine, radio wave propagation, surveillance, etc. The radar cross-section (RCS) of an object is a complicated function of observation angle, signal frequency and polarization, material and dimensions of the object. RCS may be determined by experimental measurement, but such a procedure may not be practical and applicable for all angles of observation and any object dimensions. Therefore, numerical electromagnetic techniques are required for the computation of RCS. The frequency spectrum

for RCS is divided into three regions [1, 2]: (1) Low frequency or Rayleigh region, where the object dimensions are much smaller than the wavelengths, which is attributed by its own approximation leading to the RCS being proportional to the fourth power of frequency; (2) High frequency region (or visible light), where the object dimensions are much larger than the wavelengths and high frequency techniques are successfully used for the computation of RCS, such as geometric optics (GO), physical optics (PO), geometrical theory of diffraction (GTD), uniform theory of diffraction (UTD), etc; (3) The middle frequency region or resonance region, where the object dimensions are comparable with the wavelengths and the common low frequency and high frequency approximations are not applicable. Several methods are developed for the computation of reflection coefficient and RCS of various structures [3–6]. Computation of radar cross-section in the middle frequency range requires the application of full-wave numerical techniques, such as MoM, FDTD, TLM, FEM, etc.

Several studies have been performed for the analysis of electromagnetic and optical scattering of layered cylinders composed of isotropic and anisotropic materials and also arrays of such structures in various configurations [7–11].

In this paper, we employ the fullwave theory of addition theorems for the computation of RCS for multilayered circular cylindrical objects [12–18]. The reduction of an object RCS is of interest in military and electronic warefare, which may be realized by different techniques: (1) object shaping, (2) discrete loading, (3) continuous loading, and (4) active loading. In this paper we consider the third method, which entails the usage of radar absorbing materials (RAM). Electromagnetic absorbing materials are used widely in anechoic chambers, antenna designs with low side lobe levels, electromagnetic interference protection in high speed circuits, etc. [19–21].

The design of RAM structures for reduction of RCS may be performed at a single frequency or a narrow bandwidth by Salisbury plates and Dallenbach layers, having thicknesses of a quarter wavelength [22]. To obtain wideband designs, multilayered structures are required. Although theoretical studies for the evaluation of RCS of planar structures have been extensively performed, more efforts are required in this area for other structures, such as cylinders, ellipses, spheres, wedges, cones, and their combinations.

In this paper, the computation of RCS for multilayered cylindrical objects is considered, where the number of dielectric cylindrical layers may be arbitrary. Normal plane wave incidence and both TE and TM and circular polarizations are considered. The addition theorems are employed to expand the fields as cylindrical wave

functions inside the layers and outside in free space. The numerical procedure can handle any radius of inner cylinder, any number of layers with arbitrary thicknesses, any lossless or lossy dielectric materials, arbitrary frequency bandwidth, consideration of dispersion relations and dielectric or conducting inner core cylinder.

The present study indicates several conclusions for the optimization of RCS as regards the value of permittivity and permeability of cylindrical layers, thickness of layers, frequency dependence, incident wave polarization, lossless and lossy dielectrics, etc.

The method of least squares is employed to optimize the RCS,for which the Genetic Algorithms are mainly used. At first the numerical procedure is described and then several examples and related conclusions are presented.

2. NUMERICAL PROCEDURE

Fig. 1 shows an infinitely long conducting or dielectric circular cylinder of radius 'r_1' with its axis coincident with the z axis. There are several coaxial cylindrical dielectric layers with radii 'r_2', 'r_3',.... The structure is placed in free space (ε_0, μ_0) and the time dependence is assumed as e^{-jwt}. A TE (with $E_z = 0$) or TM (with $H_z = 0$) polarized plane wave is normally incident on the multilayered cylindrical structure. The field components in cylindrical coordinates may be expressed in terms of the electric and magnetic Hertzian potentials (Π_z, Π_{mz}) for the TM

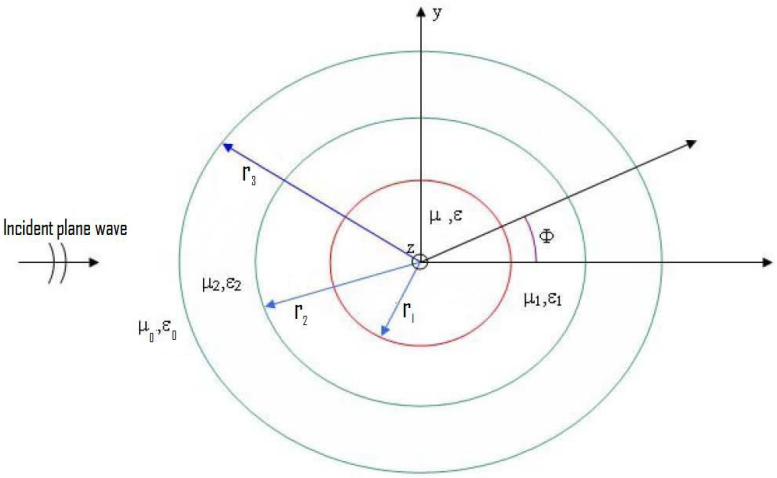

Figure 1. Geometrical configuration of the RCS problem.

and TE modes, respectively, as [23]:

$$E_z = \left[\frac{\partial^2}{\partial z^2} + K^2\right]\Pi_z, \quad H_z = \left[\frac{\partial^2}{\partial z^2} + K^2\right]\Pi_{mz} \tag{1}$$

$$E_r = \frac{\partial^2}{\partial r \partial z}\Pi_z - j\omega\mu\frac{1}{r}\frac{\partial}{\partial\varphi}\Pi_{mz} \tag{2}$$

$$E_\varphi = \frac{1}{r}\frac{\partial^2}{\partial\varphi\partial z}\Pi_z + j\omega\frac{\partial}{\partial r}\Pi_{mz} \tag{3}$$

$$H_r = j\omega\varepsilon\frac{1}{r}\frac{\partial}{\partial\varphi}\Pi_z + \frac{\partial^2}{\partial r\partial_z}\Pi_{mz} \tag{4}$$

$$H_\varphi = -j\omega\varepsilon\frac{\partial}{\partial r}\Pi_z + \frac{1}{r}\frac{\partial^2}{\partial\varphi\partial_z}\Pi_{mz} \tag{5}$$

where $K = w\sqrt{\mu\varepsilon}$ is the wave number.

The incident plane wave may be described in terms of the sum of cylindrical waves by using the addition theorem.

$$TM: \begin{cases} E_{zi} = \sum\limits_{n=-\infty}^{+\infty} j^n J_n(K_0 r) e^{jn(\varphi-\varphi_0)} \\ H_{\varphi i} = \dfrac{j}{\eta_0}\sum\limits_{n=-\infty}^{+\infty} j^n J'_n(K_0 r) e^{jn(\varphi-\varphi_0)} \end{cases} \tag{6}$$

$$TE: \begin{cases} H_{zi} = \dfrac{j}{\eta_0}\sum\limits_{n=-\infty}^{+\infty} j^n Jn(K_0 r) e^{jn(\varphi-\varphi_0)} \\ E_{\varphi i} = \sum\limits_{n=-\infty}^{+\infty} j^n J'n(K_0 r) e^{jn(\varphi-\varphi_0)} \end{cases} \tag{7}$$

where K_0 and η_0 are the wave number and intrinsic impedance of free space and φ_0 indicates the direction of incident wave. Then, the scattered fields may also be written as a sum of cylindrical waves:

$$TM: \begin{cases} E_{zs} = \sum\limits_{n=-\infty}^{+\infty} A_{ns} j^n H_n^{(1)}(K_0 r) e^{jn(\varphi-\varphi_0)} \\ H_{\varphi s} = \frac{j}{\eta_0}\sum\limits_{n=-\infty}^{+\infty} A_{ns} j^n H'^{(1)}_n(K_0 r) e^{jn(\varphi-\varphi_0)} \end{cases} \tag{8}$$

$$TE: \begin{cases} H_{zs} = \dfrac{j}{\eta_0} \displaystyle\sum_{n=-\infty}^{+\infty} B_{ns} j^n H_n^{(1)}(K_0 r) e^{jn(\varphi-\varphi_0)} \\ E_{\varphi s} = \displaystyle\sum_{n=-\infty}^{+\infty} B_{ns} j^n H'^{(1)}_n(K_0 r) e^{jn(\varphi-\varphi_0)} \end{cases} \tag{9}$$

where A_{ns} and B_{ns} are the unknown wave amplitudes, which may be determined by the boundary conditions. Now the field distribution in the l'th layer may be expressed as:

$$TM: \begin{cases} E_{zl} = \displaystyle\sum_{n=-\infty}^{+\infty} [C_{nl} J_n(K_l r) + D_{nl} Y_n(K_l r)] e^{jn(\varphi-\varphi_0)} \\ H_{\varphi l} = \dfrac{j}{\eta_l} \displaystyle\sum_{n=-\infty}^{+\infty} [C_{nl} J'_n(K_l r) + D_{nl} Y'_n(K_l r)] e^{jn(\varphi-\varphi_0)} \end{cases} \tag{10}$$

$$TE: \begin{cases} H_{zl} = \dfrac{j}{\eta_l} \displaystyle\sum_{n=-\infty}^{+\infty} [R_{nl} J_n(K_l r) + S_{nl} Y_n(K_l r)] e^{jn(\varphi-\varphi_0)} \\ E_{\varphi l} = \displaystyle\sum_{n=-\infty}^{+\infty} [R_{nl} J'_n(K_l r) + S_{nl} Y'_n(K_l r)] e^{jn(\varphi-\varphi_0)} \end{cases} \tag{11}$$

where K_l and η_l are the wave number and intrinsic impedance in the l'th layer, respectively; and where C_{nl}, D_{nl}, R_{nl} and S_{nl} are the unknown TM and TE wave amplitudes, which are determined by the imposition of boundary conditions and finally lead to the computation of electric and magnetic fields in the cylindrical layers. In case the inner cylinder of radius 'r_1' is made of perfect electric conductor (PEC), the fields inside it ($r < r_1$) are zero and in case it is made of dielectric material,the wave amplitudes 'D_{nl}', 'S_{nl}' inside it ($r < r_1$), will be zero,due to the singularity of $Y_n(K_l r)$ at $r = 0$.

Now, the continuity of tangential field components on the cylindrical boundaries at $r = r_2, r_3$,... and the vanishing of tangential electric field on the conducting surface at $r = r_1$ will lead to a set of linear equations in terms of the unknown mode coefficients. In case the inner cylinder with radius 'r_1' is made of dielectric material, the boundary conditions are the continuity of tangential field components on the surface $r = r_1$, which lead to a different set of linear equations for the mode amplitudes.

An expression for RCS may be obtained by using the large argument approximations of Hankle functions in the definition of RCS

and eqs. (8) and (9) [24].

$$TM: \frac{\sigma}{\lambda} = \frac{2}{\pi}\left|\sum_{n=-\infty}^{+\infty} A_{ns} e^{jn(\varphi-\varphi_0)}\right|^2 \tag{12}$$

$$TE: \frac{\sigma}{\lambda} = \frac{2}{\pi}\left|\sum_{n=-\infty}^{+\infty} B_{ns} e^{jn(\varphi-\varphi_0)}\right|^2 \tag{13}$$

which is the normalized bistatic RCS. For the monostatic case, we use $\varphi_0 = 0$ and $\varphi = \pi$.

3. NUMERICAL RESULTS

Several examples of optimization of RCS are considered below.

Example 1: RCS of a dielectric cylinder with a dielectric cylindrical coating
Consider a cylindrical dielectric shell with inner radius $r_1 = 0.25\lambda$ and outer radius $r_2 = 0.3\lambda$ with characteristics '$\varepsilon_r = 4,\ \mu_r = 1$'. The inner cylinder with radius 'r_1' is filled with air with '$\varepsilon_r = 1,\ \mu_r = 1$'. A TE or TM polarized plane wave is normally incident on the shell. This problem is solved in [25] by the Integral Equation Method and in [26] by the Eigenfunction Expansion Method. The RCS (σ/λ) of this structure obtained by the proposed method of addition theorems and those computed by the methods in [25] and [26] agree very well as depicted in Fig. 2 for the angle of observation from '$\varphi = 0$ to $\varphi = \pi$' for both TE and TM polarizations.

In the following examples, we consider the computation of RCS of conducting cylinders coated with several layers of dielectric materials. Examples of such structures may be the posts on ship decks.

Example 2: RCS of a conducting cylinder with a dielectric coating
Consider a conducting cylinder of radius $r_1 = 4.71\,(\text{mm})$ with a dielectric coating of $\varepsilon_r = 2.54$ having thickness '$r_2 - r_1$'. The frequency is $f = 9.57\,\text{GHz}$ with the wave number in free space ($K_0 = 200$) and that in the dielectric (K_1). The normalized RCS (*namely* σ/λ_0) is computed and plotted versus ($K_1 r_2$) at a single frequency in Fig. 3, and compared with the experimental results in [27].

Another example is shown in Fig. 4, where its data are given in the caption. Excellent agreement may be seen between the RCS computation by the proposed method and the measurement data in [27].

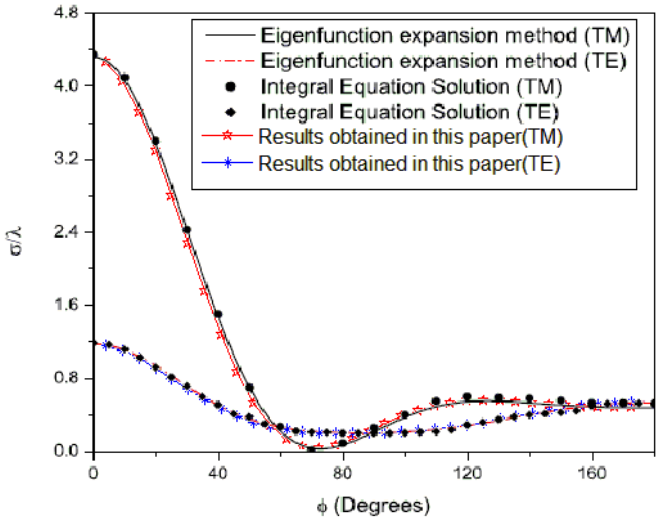

Figure 2. Analytical results (Addition theorem) of RCS of a dielectric cylindrical shell for TM and TE polarizations compared with the Integral Equation Method results [25] and by the Eigenfunction Expansion Method results [26].

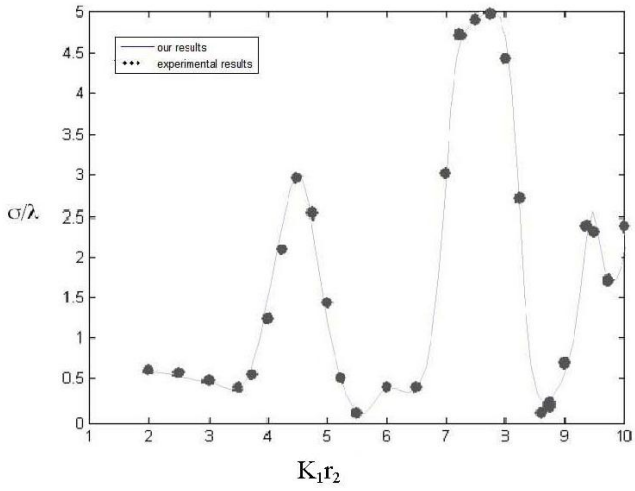

Figure 3. Analytical results (our results) of normalized radar cross-section of a nonmagnetic dielectric coated cylinder for TM polarization compared with experimental results by Tang [27].

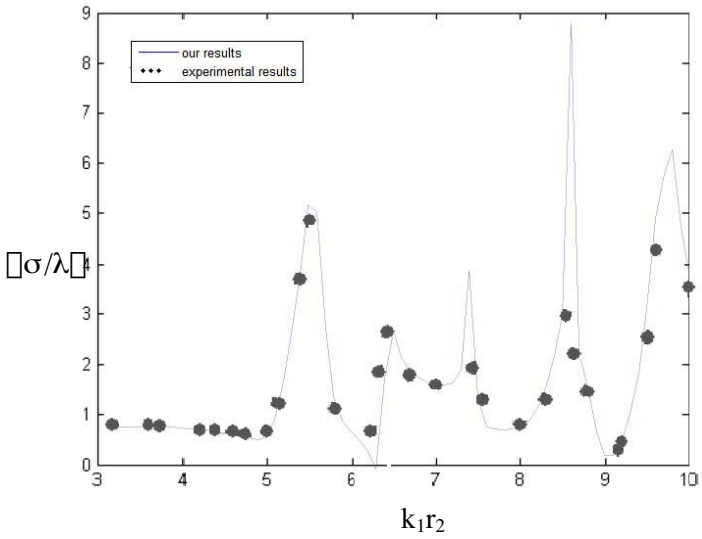

Figure 4. Analytical results (our results) of normalized RCS of a conducting cylinder ($r_1 = 6.51\,\text{mm}$) with a dielectric coating ($\varepsilon_r = 6$) at frequency $f = 9.57\,\text{GHz}$ for TM polarization.

For the optimization of RCS, the method of least squares is used [28]. The specified frequency bandwidth is divided into n_f discrete frequencies. Then an error function is constructed as:

$$Error = \sum_{i=1}^{n_f} W_i (\frac{\sigma_i}{\lambda} - c_i)^2 \tag{14}$$

where c_i is the desired value of RCS at frequency f_i. If our objective is to minimize RCS equally at all frequencies, then $c_i = 0$.

W_i is the weighting function for frequency f_i, which strengthens or weakens the corresponding term with respect to the other terms.

In the following examples, several parameters are kept the same, such as the radius of inner conducting cylinder which is kept constant at $r_1 = 50\,\text{mm}$, number of modes $N = 50$, bandwidth $f_1 = 1\,\text{GHz}$ to $f_2 = 10\,\text{GHz}$, number of discrete frequencies $n_f = 70$.

The thickness of layers is constrained between 0.1 mm and 30 mm.

The values of relative permittivity and permeability are constrained between 1 and 30 in several examples and between 0.01 and 30 in other examples.

The radius of inner PEC cylinder is kept constant but the thickness (t) of layers and their permittivity (ε) and permeability (μ)

are allowed to vary in the optimization procedure to arrive at the optimum RCS.

The optimum values of t, ε and μ are determined after several runs of the Genetic Algorithm on the main program of RCS. We consider one layer and two layer dielectric coatings.

Example 3: Minimization of RCS of PEC cylinder with one coating layer and TE polarization

Optimization of the normalized RCS versus frequency is shown in Fig. 5 for three cases:

$$\begin{cases} a: & \text{no coating} \\ b: & \text{with magnetic coating } t_1 = 0.12\,(\text{mm}), \varepsilon_{r_1} = 33.78,\ \mu_{r_1} = 31.6 \\ c: & \text{with nonmagnetic coating } t_1 = 14.68\,(\text{mm}),\ \varepsilon_{r_1} = 3.57, \mu_{r_1} = 1 \end{cases} \tag{15}$$

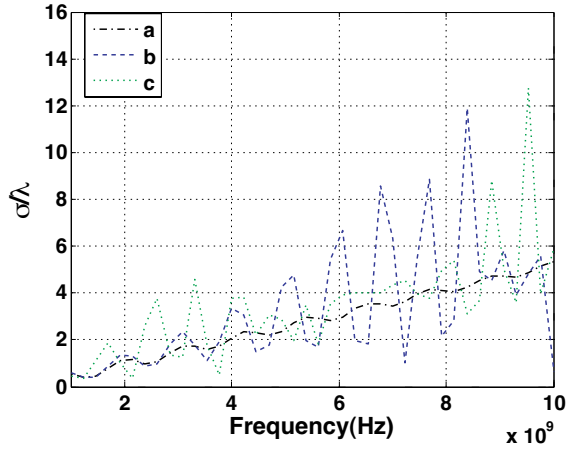

Figure 5. Normalized RCS of a coated conducting cylinder ($r_1 = 50\,\text{mm}$) for TE polarization for the three cases specified in example 3.

It is observed that RCS of PEC cylinder with coating becomes very oscillatory and at some frequencies increases sharply. Consequently, it seems that in this case dielectric coating is useless for reduction of RCS. However, the minimum value of error function as the sum of squares of RCS over the frequency bandwidth remains the same, although the coating characteristics differ. It is seen that the magnetic coating is thinner than the nonmagnetic one for the minimization of RCS.

It is possible to significantly reduce RCS at a single frequency by the application of coating. For example, at $f = 10\,\text{GHz}$, no coating: $\frac{\sigma}{\lambda} = 5.34$, with coating: $t_1 = 0.12\,(\text{mm}),\ \varepsilon_r = 33.77,\ \mu_r = 31.6,\ \frac{\sigma}{\lambda} =$

0.656

Example 4: Minimization of RCS of a conducting cylinder ($r_1 = 50\,$mm) with one coating layer and TM polarization
Minimization of the normalized RCS versus frequency is shown in Fig. 6, for three cases:

$$\begin{cases} a: \text{ no coating} \\ b: \text{ with magnetic coating, } t_1 = 2.34\,(\text{mm}),\ \varepsilon_{r_1} = 16.35,\ \mu_{r_1} = 30.50 \\ c: \text{ with nonmagnetic coating, } t_1 = 12.41\,(\text{mm}),\ \varepsilon_{r_1} = 17.19,\ \mu_{r_1} = 1 \end{cases} \tag{16}$$

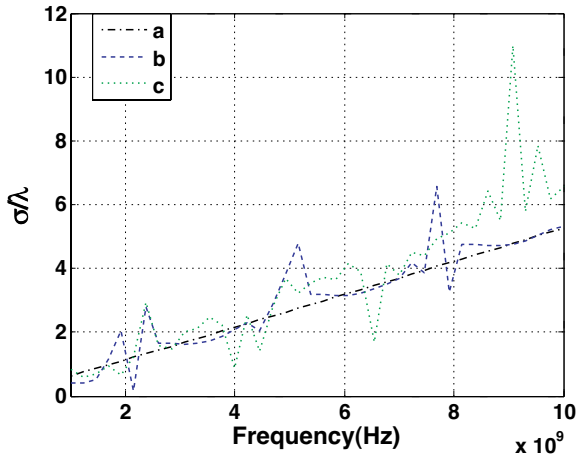

Figure 6. Normalized RCS of a coated conducting cylinder ($r_1 = 50\,$mm) for TM polarization for the three cases specified in example 4.

Example 5: Minimization of RCS of a conducting cylinder ($r_1 = 50\,$mm) with one coating layer with $0 < \varepsilon_r < 1$, and $0 < \mu_r < 1$ and TE polarization
Minimization of RCS versus frequency is shown in Fig. 7 for four cases:

$$\begin{cases} a: & \text{no coating} \\ b: & \text{with coating, } t_1 = 5\,(\text{mm}),\ \varepsilon_{r_1} = 0.02,\ \mu_{r_1} = 0.06 \\ c: & \text{with coating and 'bandwidth 3–5 GHz',} \\ & t_1 = 14.5\,(\text{mm}), \varepsilon_{r_1} = 0.05,\ \mu_{r_1} = 0.14 \\ d: & \text{with coating, } t_1 = 27\,(\text{mm})\ \varepsilon_{r_1} = 0.0852,\ \mu_{r_1} = 0.0523 \end{cases} \tag{17}$$

The scale for RCS is logarithmic ($10\log\frac{\sigma}{\lambda}$) to better show the value of RCS and its reduction through minimization. It is seen that

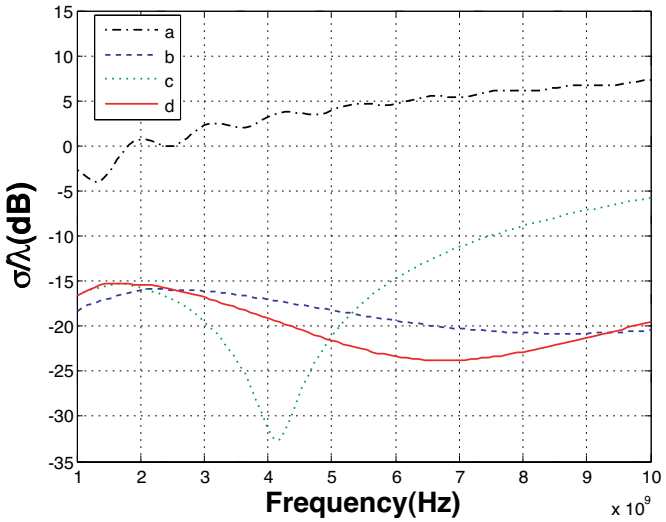

Figure 7. Normalized RCS in dB of a coated conducting cylinder ($r_1 = 50\,\text{mm}$ and $0 < \varepsilon_r < 1$) with TE polarization for the four cases specified in example 5.

application of coating drastically reduces RCS. However, optimum values of RCS depend on the assumed frequency bandwidth, which is evident for optimum case (c) in Fig. 7.

Example 6: Minimization of RCS of a conducting cylinder ($r_1 = 50\,\text{mm}$) with one coating layer with $0 < \varepsilon_1 < 1$, and TM polarization

Minimization of RCS versus frequency is shown in Fig. 8 for three cases:

$$\begin{cases} a: \text{ no coating} \\ b: \text{ with coating, } t_1 = 0.2\,(\text{mm}),\ \varepsilon_{r_1} = 0.02,\ \mu_{r_1} = 40 \\ c: \text{ with coating, } t_1 = 0.5\,(\text{mm}),\ \varepsilon_{r_1} = 0.15,\ \mu_{r_1} = 1 \end{cases} \tag{18}$$

It is seen that reduction of RCS for TM polarization is not possible in a wide frequency bandwidth by the application of one layer material coating. However, reduction of RCS is achieved at a single frequency or a narrow bandwidth. For example, at $f = 5\,\text{GHz}$

$$\begin{cases} d: & \text{no coating, } \frac{\sigma}{\lambda} = 2.67 \\ e: & \text{with coating, } t_1 = 30\,(\text{mm}),\ \varepsilon_{r_1} = 0.0544, \\ & \mu_{r_1} = 18.249, \frac{\sigma}{\lambda} = 0.0023 \end{cases} \tag{19}$$

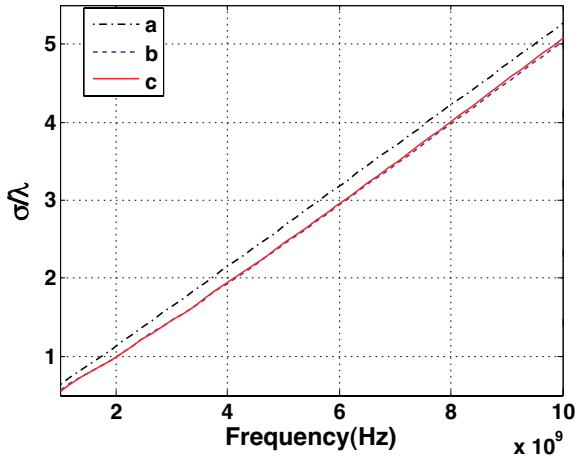

Figure 8. Normalized RCS of a coated conducting cylinder (r_1 = 50 mm) and ($0 < \varepsilon_r < 1$) for TM polarization for the three cases specified in example 6.

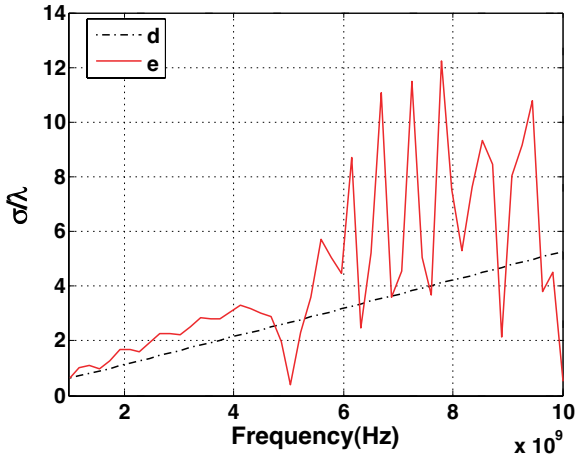

Figure 9. Normalized RCS of a coated conducting cylinder (r_1=50 mm) for TM polarization, minimized at 5 GHz compared with an uncoated one (example 6).

The variation of RCS versus frequency is shown in Fig. 9.

It is seen that RCS is reduced at $f = 5$ GHz, but at the expense of its increase at other frequencies.

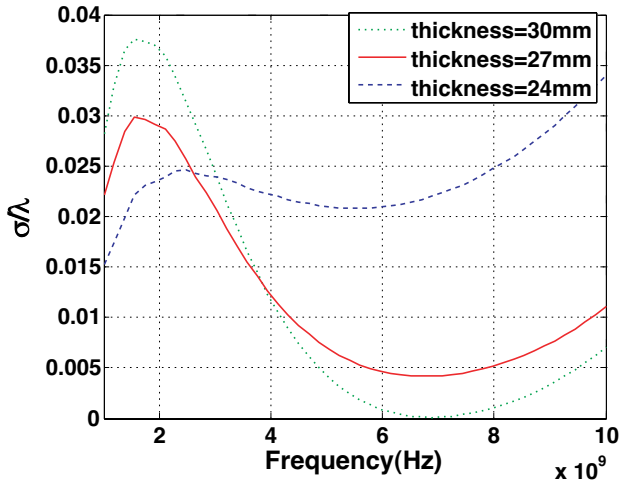

Figure 10. Sensitivity of RCS to variation of the coating thickness for TE polarization.

Sensitivity of RCS with respect to parameters t, ε_r and μ_r
Consider the optimum case in Fig. 7 for TE polarization and $t = 27\,(\text{mm})$. Now consider the same values for ε_r and μ_r, but change the coating thickness by about $\pm 10\%$. Values of RCS are drawn for $t = 24\,(\text{mm})$ and $t = 30\,(\text{mm})$ in Fig. 10.

It is observed that RCS changes drastically and it is very sensitive to coating thickness for TE polarization.

Then consider the optimum case in Fig. 8. For TM polarization the values of RCS are computed for coating thicknesses $t = 0.1, 0.5, 0.9, 2.5\,(\text{mm})$ and drawn versus frequency in Fig. 11. It is seen that RCS is quite insensitive to coating thicknesses, which is due to the fact that the coating material is lossless and that the electric field component is parallel to the axis of conducting cylinder.

Next, we study the sensitivity of RCS with respect to permittivity (ε_r) of coating material. Consider the optimum case of TE polarization with $\varepsilon_r = 0.0852$ in Fig. 7 and change ε_r by about $\pm 10\%$. The values of RCS are drawn in Fig. 12 for $\varepsilon_r = 0.1$, $\varepsilon_r = 0.065$ and $\varepsilon_r = 0.0852$, which show its high sensitivity to ε_r.

Now, consider the optimum case for TM polarization with $\varepsilon_r = 0.15$ in Fig. 8. The values of RCS are drawn in Fig. 13 for $\varepsilon_r = 0.03, 0.15, 0.27$ and 1.5, which show its very low sensitivity to ε_r.

The sensitivity of RCS with respect to the values of μ_r (for TE and TM polarizations of incident wave) is similar to that of ε_r.

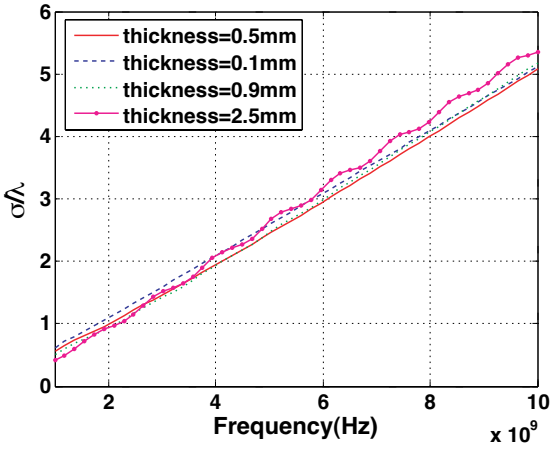

Figure 11. Sensitivity of RCS to variation of the coating thickness for TM polarization

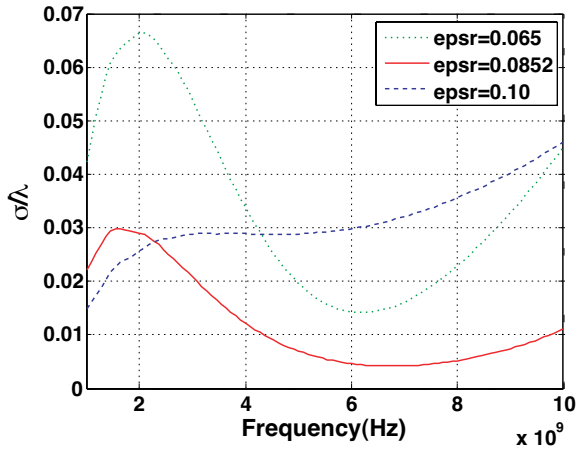

Figure 12. Sensitivity of RCS to variation of the coating permittivity for TE polarization.

Example 7: Reduction of RCS of a conducting cylinder ($r_1 = 50\,\mathbf{mm}$) with two coating layers with TE polarization
First, we consider common materials with $\varepsilon_r > 1$ and $\mu_r > 1$. RCS is

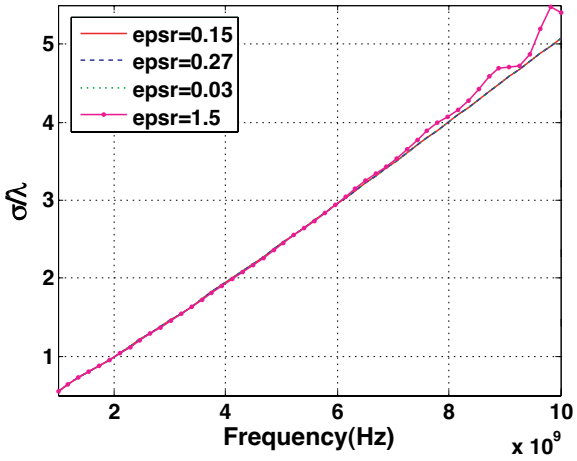

Figure 13. Sensitivity of RCS to variation of the coating permittivity for TM polarization.

drawn versus frequency in Fig. 14 for the following cases:

$$\begin{cases} a: & \text{no coating} \\ b: & \text{first layer, } t_1 = 29.9\,(\text{mm}),\ \varepsilon_{r_1} = 1.0017,\ \mu_{r_1} = 2.3167 \\ & \text{second layer, } t_2 = 0.285\,(\text{mm}),\ \varepsilon_{r_2} = 1.01194,\ \mu_{r_2} = 2.3374 \\ c: & \text{first layer, } t_1 = 11.2\,(\text{mm}),\ \varepsilon_{r_1} = 0.0414,\ \mu_{r_1} = 0.1296 \\ & \text{second layer, } t_2 = 0.4\,(\text{mm}),\ \varepsilon_{r_1} = 3.5764,\ \mu_{r_2} = 1.3639 \end{cases} \tag{20}$$

It is observed that common materials $\varepsilon_r,\ \mu_r > 1$ are not effective in reducing RCS. However, special materials ($\varepsilon_r < 1, \mu_r < 1$ or $\mu_r > 1$) are capable of drastically reducing RCS.

Example 8 : Reduction of RCS due to a conducting cylinder (r_1=50 mm) with two coating layers with TM polarization
Again, reduction of RCS is not possible by common materials. However, materials with $0 < \varepsilon_r, \mu_r < 1$ achieve this objective. Fig. 15 shows RCS versus frequency for the cases of no coating (a) and the following optimum characteristics (b):

$$\begin{cases} \text{first layer, } t_1 = 22.02\,(\text{mm}),\ \varepsilon_{r_1} = 0.014,\ \mu_{r_1} = 26.38 \\ \text{second layer, } t_2 = 5.8\,(\text{mm}),\ \varepsilon_{r_2} = 0.0575,\ \mu_{r_2} = 0.0155 \end{cases} \tag{21}$$

The above examples have used lossless dielectrics, which lead to the reduction of RCS not by electromagnetic energy losses but through its diversion towards other directions than the transmitting antenna.

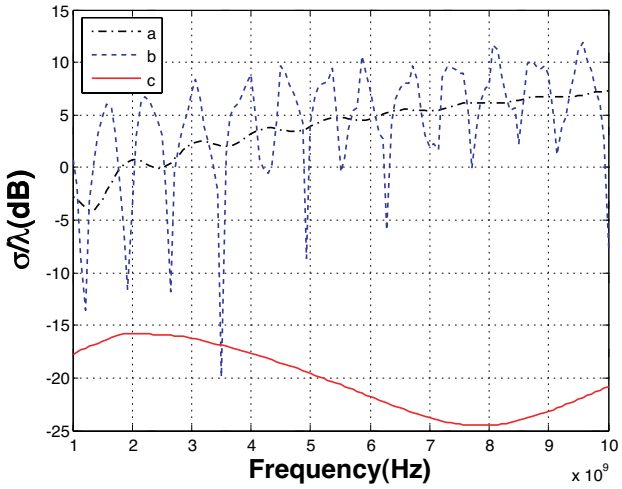

Figure 14. Normalized RCS (in dB scale) of a two layer coated conducting cylinder ($r_1 = 50\,\text{mm}$) for TE polarization in the three cases specified in example 7.

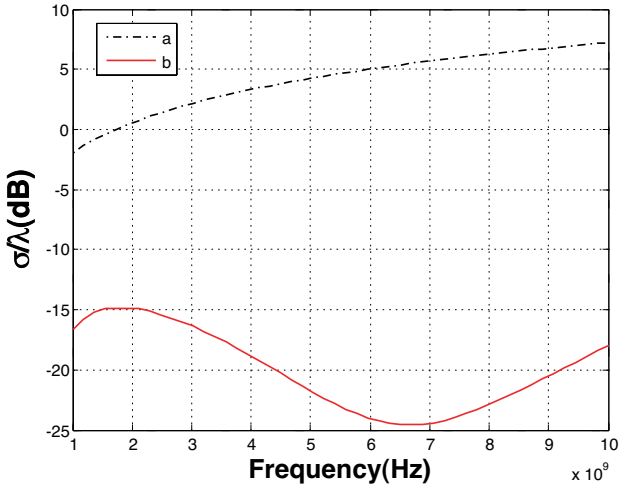

Figure 15. Normalized RCS (in dB scale) of a two layer coated conducting cylinder ($r_1 = 50\,\text{mm}$) for TM polarization in the two cases specified in example 8.

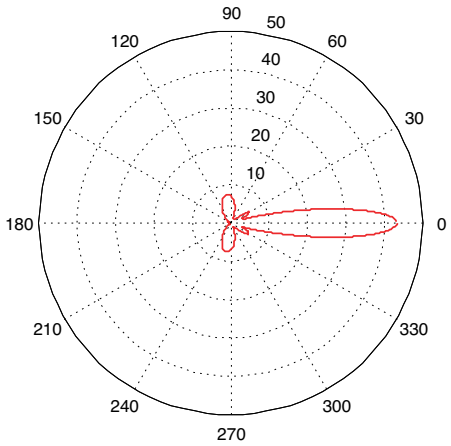

Figure 16. Normalized RCS of a two layer coated conducting cylinder ($r_1 = 50\,\text{mm}$) with respect to angle phi at 6 GHz and TE polarization for minimum RCS case.

The polar plot of normalized RCS is drawn in Fig. 16, for the optimum case of a conducting cylinder (radius $r_1 = 50$ mm) with two layers of coating with TE polarization.

It is seen that backward scattering is minimized but the transmitted signal energy is directed towards forward scattering.

The proposed method may be used to compute RCS of the coated conducting cylinder in any direction and optimize it.

Example 9: Maximizing RCS of a conducting cylinder ($r_1 = 50\,\text{mm}$) with two coating layers with TE polarization

There may be occasions to increase the RCS of an object, such as recreational ships and trackable objects. For example, RCS of a cylinder with no coating and its maximum and minimum RCS's with two layers of coating are drawn in Fig. 17 versus frequency.

minimum RCS

$$\begin{cases} \text{first layer, } t_1 = 11.2\,(\text{mm}),\ \varepsilon_{r_1} = 0.0414,\ \mu_{r_1} = 0.1296 \\ \text{second layer, } t_2 = 0.4\,(\text{mm}),\ \varepsilon_{r_2} = 3.5764,\ \mu_{r_2} = 1.3639 \end{cases} \tag{22}$$

maximum RCS

$$\begin{cases} \text{first layer, } t_1 = 28.9\,(\text{mm}),\ \varepsilon_{r_1} = 12.6683,\ \mu_{r_1} = 0.1746 \\ \text{second layer, } t_2 = 0.108\,(\text{mm}),\ \varepsilon_{r_2} = 11.0558,\ \mu_{r_2} = 25.4616 \end{cases} \tag{23}$$

The variation of maximum RCS is very oscillatory. The polar plot of maximum RCS is shown in Fig. 18, where the backscattered wave is relatively high.

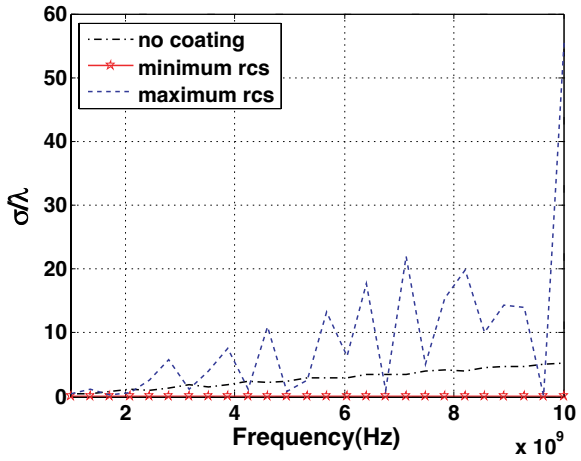

Figure 17. Normalized RCS of a two layer coated conducting cylinder ($r_1 = 50\,\text{mm}$) for TE polarization in three cases : a) no coating, b) minimum RCS, c) maximum RCS in example 9.

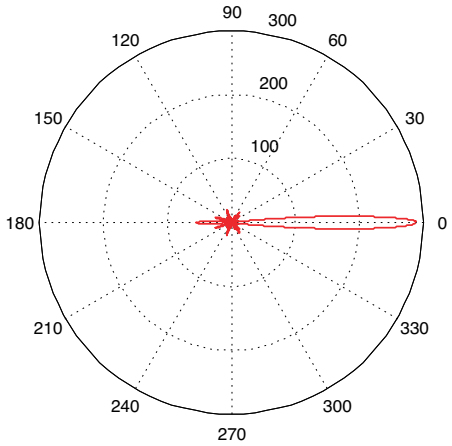

Figure 18. Normalized RCS of a two layer coated conducting cylinder ($r_1 = 50\,\text{mm}$) with respect to angle phi at 10 GHz and TE polarization in maximum RCS case.

The maximum RCS of the two layer coating is

$$\frac{\sigma}{\lambda}|_{f=10\,\text{GHZ}} = 55.6 \tag{24}$$

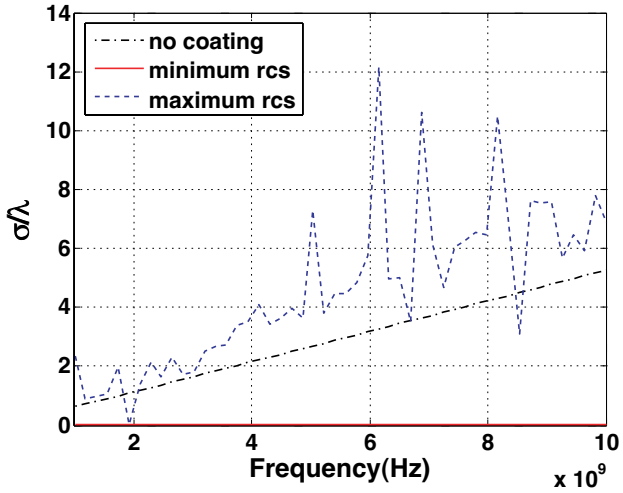

Figure 19. Normalized RCS of a two layer coated conducting cylinder ($r_1 = 50\,\text{mm}$) for TM polarization in three cases: a) no coating, b) minimum RCS, c) maximum RCS in example 10.

and that with no coating

$$\frac{\sigma}{\lambda}|_{f=10\,\text{GHZ}} = 5.33 \tag{25}$$

Example 10: Maximizing RCS of a conducting cylinder (r_1=50 mm) with two coating layers with TM polarization
The RCS of the cylinder with no coating, the minimum and maximum RCS's of the cylinder with two layers of coating are shown in Fig. 19.

$$\begin{array}{l} \textit{minimum} \quad \textit{RCS} \\ \left\{ \begin{array}{l} \text{first layer, } t_1 = 22.02\,(\text{mm}),\ \varepsilon_{r_1} = 0.014,\ \mu_{r_1} = 26.38 \\ \text{second layer, } t_2 = 5.8\,(\text{mm}),\ \varepsilon_{r_2} = 0.0575,\ \mu_{r_2} = 0.0155 \end{array} \right. \end{array} \tag{26}$$

$$\begin{array}{l} \textit{maximum} \quad \textit{RCS} \\ \left\{ \begin{array}{l} \text{first layer, } t_1 = 19.5\,(\text{mm}),\ \varepsilon_{r_1} = 16.5266,\ \mu_{r_1} = 1.6456 \\ \text{second layer, } t_2 = 13.7\,(\text{mm}),\ \varepsilon_{r_2} = 5.2877,\ \mu_{r_2} = 20.3588 \end{array} \right. \end{array} \tag{27}$$

The curve of maximum RCS for coated cylinder is generally above that of the uncoated cylinder, except at two frequencies 1.918 GHz and 8.6 GHz.

Example 11: Reduction of RCS of a conducting cylinder ($r_1 = 50\,$mm) with a layer of lossy coating for TE polarization

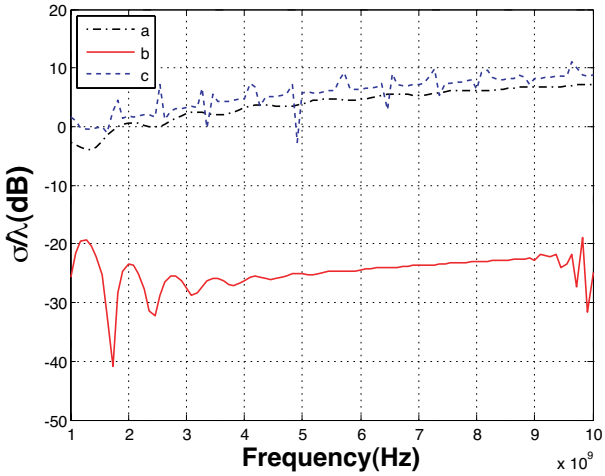

Figure 20. A comparison of normalized RCS of a single layer coated cylinder for TE polarization in three cases: a) no coating, b) minimum RCS by lossy coating, c) RCS by lossless coating in example 11.

Now, we consider lossy materials for coating layers by assuming complex permittivity and permeability. We observed that common lossless materials (with $\varepsilon_r,\ \mu_r > 1$) are not effective for reduction of RCS. However, for comparison we use here complex ε and μ, with real parts greater than unity. Here frequency dispersion is ignored. The minimum values of RCS are drawn in Fig. 20, for a cylinder with no coating and with a single layer of coating:

$$\begin{cases} a: & \text{no coating} \\ b: & \text{with lossy coating: } t_1 = 28.7\,(\text{mm}), \\ & \varepsilon_{r_1} = 6.2955 + j1.697,\ \mu_{r_1} = 7.106 + j1.615 \\ c: & \text{with lossless coating: } t_1 = 28.7\,(\text{mm}), \varepsilon_{r_1} = 6.2955, \mu_{r_1} = 7.106 \end{cases} \tag{28}$$

For comparison the values of RCS are also computed for the above parameters, but taking only the real parts of ε_r and μ_r. It is seen that lossy dielectric coatings drastically decrease RCS.

Example 12: Reduction of RCS of a conducting cylinder (r_1=50 mm) with a layer of lossy coating for TM polarization
As it was seen before, reduction of RCS for TM polarization was not possible by common lossless materials (for both ε_r and μ_r greater or smaller than unity). Therefor, we consider lossy materials for the

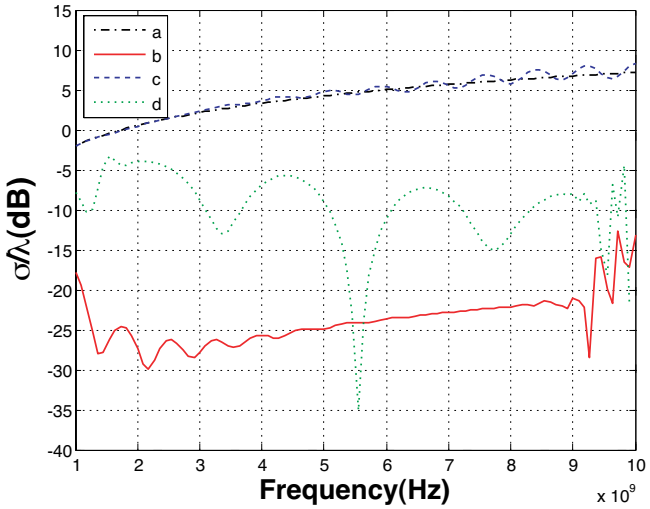

Figure 21. A comparison of normalized RCS of a one layer coated cylinder for TM polarization in four cases : a) no coating b) minimum RCS by lossy coating c) RCS by lossless coating d) minimum RCS by a relatively narrow lossy coating in example 12.

coating and minimize RCS for TM polarization as shown in Fig. 21. For comparison minimum values of RCS are drawn for the case of no coating. The minimization of RCS with one layer of lossy coating drastically decreases its value and provides the following parameters:

$$\begin{cases} a: & \text{no coating} \\ b: & \text{with lossy coating: } t_1 = 29.3\,(\text{mm}), \\ & \varepsilon_{r_1} = 1.281 + j1.701,\ \mu_{r_1} = 1.011 + j1.807 \\ c: & \text{with lossless coating: } t_1 = 29.3\,(\text{mm}), \varepsilon_{r_1} = 1.281,\ \mu_{r_1} = 1.011 \end{cases} \tag{29}$$

Again, if the imaginary parts of ε_r and μ_r are ignored, no reduction of RCS is observed by applying the coating. As the thickness of lossy layer of coating increases, its dissipation also increases which leads to the attenuation of the reflected waves. Accordingly, the thickness of the lossy layer is fixed at $t = 5\,(\text{mm})$ and RCS is minimized and drawn in Fig. 21.

$$d: \text{with lossy coating: } t_1 = 5\,(\text{mm}),\ \varepsilon_{r_1} = 17.932 + j1.709,\ \mu_{r_1} = 10.34 + j1.688 \tag{30}$$

It is seen that the RCS curve for thin coating is located above that of the optimum case.

3-D diagrams

In order to observe the complication of optimization processes, the RCS is drawn at a single frequency as the function of ε_r and μ_r. For example, consider the conducting cylinder of radius $r_1 = 50\,(\text{mm})$ with one lossless layer of thickness $t = 1\,(\text{mm})$, at frequency $f = 5(\,\text{GHz})$ and TE polarization. The values of RCS are drawn versus values of ε_r and μ_r in Fig. 22.

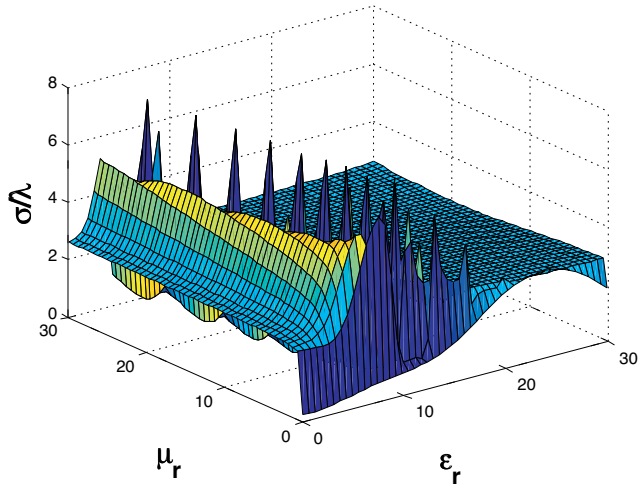

Figure 22. 3D diagram of normalized RCS of a conducting cylinder with a thin layer coating ($t = 1\,\text{mm}$) for TE polarization at frequency $5\,\text{GHz}$.

It is seen that for thinner layers ($\frac{t}{\lambda} = \frac{1}{60}$), the variations of RCS is quite smooth. However, for thicker layers ($\frac{t}{\lambda} = \frac{5}{6}$), the variations of RCS are quite rapid and sharp, as seen in Fig. 23. The number of extrema is quite high. This situation makes the convergence towards the global minimum quite difficult.

Incident plane wave with circular polarization

Now, we consider the normal incidence of a circularly polarized plane wave on to a conducting cylinder having several layers of dielectric material. We would like to minimize its RCS. Consider the circularly polarized plane wave [29]:

$$\bar{E}_{ti} = (E_{\varphi i}\hat{\varphi}_-^+ jE_{zi}\hat{z}) = E_0 e^{-jkr}(\hat{\varphi}_-^+ j\hat{z}) \tag{31}$$

where signs + and − indicate right-handed and left-handed polarized plane waves, respectively, which are composed of TE and TM modes.

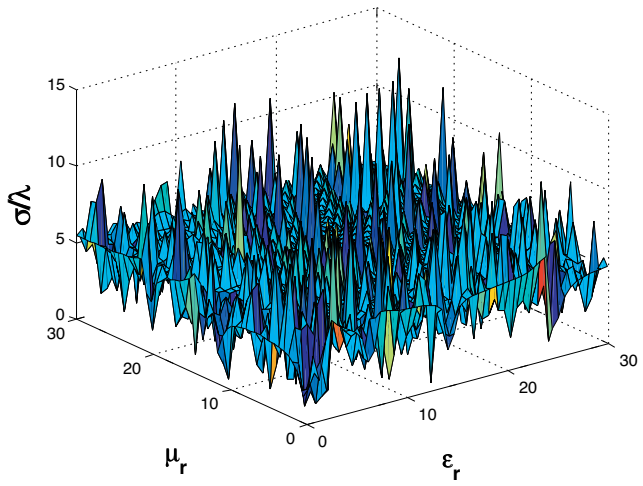

Figure 23. 3D diagram of normalized RCS of a conducting cylinder with a thick layer coating ($t = 50\,\text{mm}$) for TE polarization at frequency 5 GHz.

Since the reflection amplitudes of TE and TM modes are different the reflected wave will generally have elliptic polarization. That is,

$$\bar{E}_{ts} = (E_{\varphi s}\hat{\varphi}_{+}^{-} j E_{zi}\hat{z}) \tag{32}$$

The radar cross-section(RCS) of two dimensional structures is calculated by

$$RCS = \lim_{r\to\infty} 2\Pi r \frac{|E_{ts}|^2}{|E_{ti}|^2} \tag{33}$$

However, we have

$$\begin{aligned} |E_{ts}|^2 &= |E_{\varphi s}|^2 + |E_{zs}|^2 \\ |E_{ti}|^2 &= |E_{\varphi i}|^2| + E_{zi}|^2 = 2E_0^2 \end{aligned} \tag{34}$$

We may recall that TE and TM polarizations are completely decoupled for normal plane wave incidence on a multilayered conducting cylinder. Therefore, they may be analyzed separately and the resultant reflected wave may be obtained as the superposition of the individual cases. Consequently, RCS may be computed by eq. (33).

Example 13: Minimization of RCS of a conducting cylinder ($r_1 = 50\,\text{mm}$) with one coating layer and circular polarization Consider a conducting cylinder of radius $r_1 = 5\,\text{cm}$ with one lossless

layer coating under normally incident circularly polarized plane wave. Minimization of RCS leads to the following parameters for the layer: Thickness, $t_1 = 2.2\,(\text{mm}),\ \varepsilon_{r_1} = 0.014,\ \mu_{r_1} = 1$.

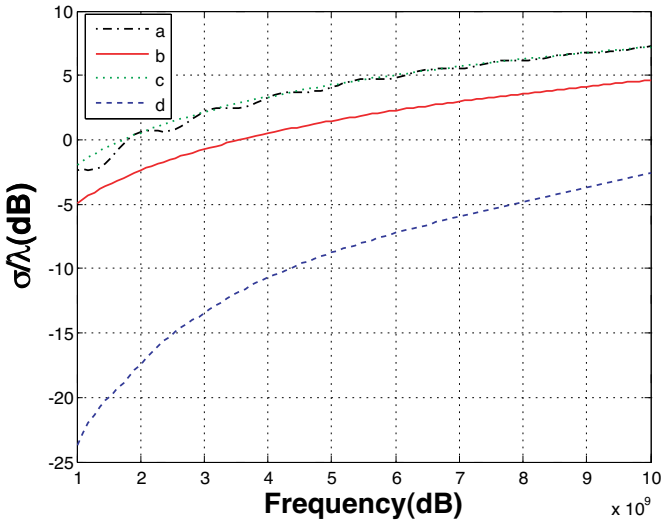

Figure 24. Normalized RCS (in dB scale) of a single layer coated conducting cylinder ($r_1 = 50\,\text{mm}$) for TE (d), TM (c) and circular polarizations (b) compared with a bare cylinder (a) in example 13.

RCS is drawn in Fig. 24, for TE (d), TM (c), and circularly polarized plane waves (b) and also for the case of no coating for circularly polarized plane wave (a). As expected, the RCS curve for TM polarization (with coating) is close to that of the case with no coating, and also that of the circular polarization is relatively close to them. However, in comparison, reduction of RCS for TE polarization with coating is quite evident.

Example 14 : Reduction of RCS of a conducting cylinder (r_1=50 mm) with two coating layers with circular polarization Here the same problem as example 13 is considered, but there are two layer coatings. The minimization of RCS leads to the following parameters for the two layers.

$$\begin{cases} \text{first layer, } t_1 = 3.1\,\text{mm},\ \varepsilon_{r_1} = 0.0120,\ \mu_{r_1} = 1.4179 \\ \text{second layer, } t_2 = 29.7\,\text{mm},\ \varepsilon_{r_2} = 0.1977,\ \mu_{r_2} = 0.0791 \end{cases} \tag{35}$$

For comparison RCS is drawn for TE (d), TM (c) and circular polarizations (b) and also for the case of no coating for circularly

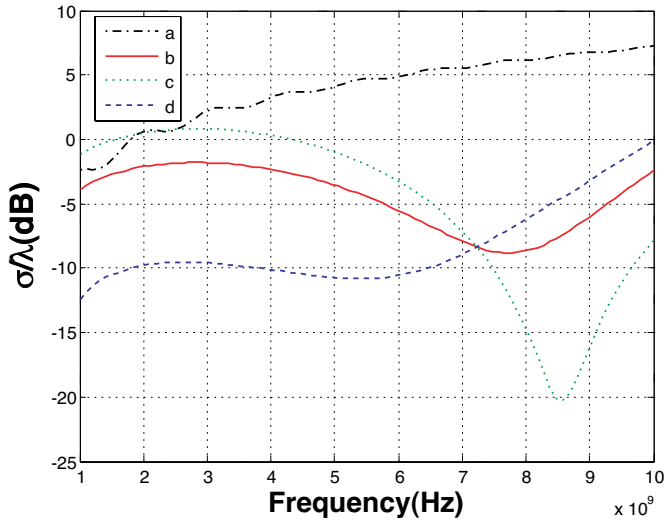

Figure 25. Normalized RCS (in dB scale) of a two layer coated conducting cylinder ($r_1 = 50\,\text{mm}$) for TE (d), TM (c) and circular polarizations (b) compared with a bare cylinder (a) in example 14.

polarized plane wave (a) in Fig. 25 The RCS curve for circular polarization lies between those of TE and TM polarizations.

Example 15: Reduction of RCS of a conducting cylinder (r_1=50 mm) with a layer of lossy coating for circular polarization

Here the same problem as example 13 is considered, but the single coating layer is assumed to be lossy. The minimization of RCS leads to the following parameters:

$$t_1 = 3\,\text{mm},\ \varepsilon_{r_1} = 3.4573 + j1.8926,\ \mu_{r_1} = 3.5291 + j1.4691$$

For comparison, in Fig. 26, RCS curves are drawn for TE (d), TM (c) and circular polarizations (b) and also for the case of no coating for circularly polarized plane wave (a). It is observed that the minimization of RCS leads to the same values for TE, TM and circular polarizations at high frequencies. However, circular polarization is commonly used for radar applications. For thin cylinders, the value of RCS is very small for TE polarization and any reflections from the thin cylinders are mainly due to the TM polarized waves.

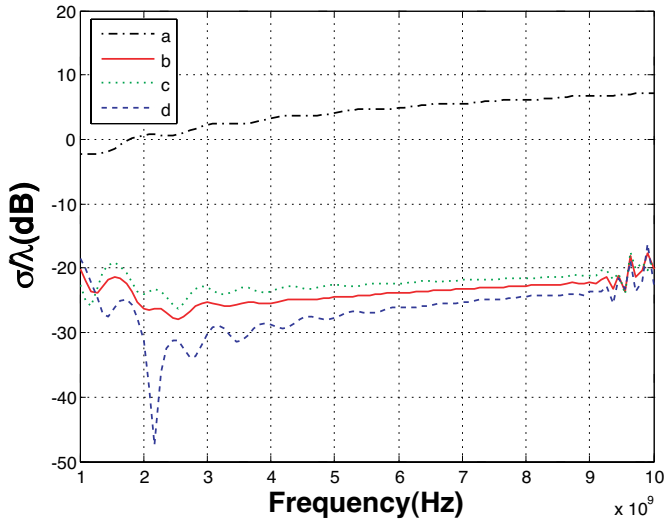

Figure 26. Normalized RCS (in dB scale) of a lossy material coated conducting cylinder ($r_1 = 50\,\text{mm}$) for TE (d), TM (c) and circular polarizations (b) compared with bare cylinder (a).

4. CONCLUSIONS

In this paper, the addition theorems are applied to analyze normal incidence of plane waves onto infinitely long dielectric layered cylinders. Particularly, uncoated conducting cylinders and one and two layers of dielectric coatings have been considered. TE, TM and circularly polarized normally incident plane waves were considered. The main objectives have been to minimize or maximize the radar cross-section (RCS) by the method of least squares. Since electromagnetic scattering is highly dependent on frequency, it has been observed that reduction of RCS may not be achievable in a wide frequency bandwidth by using solely common dielectric materials, (with $\varepsilon_r,\ \mu_r > 1$), whereas a combination of common dielectrics and unconventional materials (with $0 < \varepsilon_r,\ \mu_r < 1$) are required for coatings to minimize RCS. For TE polarization, one dielectric coating layer may be sufficient. However, for TM polarization, one layer (with any value of ε_r and μ_r) may not be adequate and two or more coating layers are required. In these cases, the reduction of RCS in the direction of transmitters is achieved mainly by diverting the reflected wave towards other directions application of materials (with $\varepsilon_r,\ \mu_r > 1$) may lead to the reduction of RCS in a narrow frequency bandwidth or at a single frequency, but it can not

do so in a broad frequency bandwidth. In general, reduction of RCS at a frequency may lead to the increase of RCS at other frequencies.

The sensitivity of RCS with respect to the variation of parameters, such as layer thicknesses, permittivities and permeabilities is drastic for the TM polarization than for the TE polarization. As the thicknesses of dielectric layers increase, the rate of variation of RCS with respect to the variations of ε and μ becomes more intense.

In the cases where the dielectric layers are lossless, the reduction of RCS in a particular direction is mainly due to the diversion of electromagnetic ways towards other directions than that of the transmitter. Evidently, RCS may be reduced by using lossy dielectric coatings, which leads to the absorption of radar signal energy in the object. On the contrary, it has been shown that maximization of RCS is also possible by designing dielectric coating layers on the cylindrical core.

Reduction of RCS for circular polarization is actually achieved by its reduction for both TE and TM linear polarizations. Consequently the reduction of RCS for circular polarization is quite hard. Thus, radars usually use circularly polarized signals. The dispersion relations for lossy dielectrics, lossy magnetics, relaxation type magnetics, etc. may readily be incorporated in the formulations and numerical procedure to better model the RCS reduction. It has been observed that relaxation type magnetics are more effective in reducing RCS. Figs. 22 and 23 show that RCS of the multilayerd cylindrical structure is a complicated function of permittivity, permeability, thickness and radius of cylindrical shells in the frequency spectrum. However, such relationships are even more complicated in the middle frequency band(relative to the dimensions of the cylindrical structure).

REFERENCES

1. Knot, E. F., J. F. Shaeffer, and M. T. Tuley, *Radar Cross-Section,* Artech House, Norwood, MA, 1986.
2. Skolnik, M. I., *Radar Handbook,* McGrawhill, NY, 1986.
3. Oraizi, H. and M. Afsahi, "Analysis of planar dielectric multilayers as Fss by transmission line transfer matrix method (TLTMM)," *Progress In Electromagnetics Research*, PIER 74, 217–240, 2007.
4. Vinogradov, S. S., P. D. Smith, J. S. Kot, and N. Nikolic, "Radar cross-section studies of spherical lens reflectors," *Progress In Electromagnetics Research*, PIER 72, 325–337, 2007.

5. Fabbro, V., P. F. Combes, and N. Guillet, "Apparent radar cross section of a large target illuminated by a surface wave above the sea," *Progress In Electromagnetics Research*, PIER 50, 41–60, 2005.
6. El-Ocla, H., "On laser radar cross section of targets with large sizes for E-polarization," *Progress In Electromagnetics Research*, PIER 56, 323–333, 2006.
7. Zhang, M., T. S. Yeo, L. W. Li, and M. S. Leong, "Electromagnetic scattering by a multilayer gyrotropic bianisotropic circular cylinder," *Progress In Electromagnetics Research*, PIER 40, 91–111, 2002.
8. Yang, J., L. W. Li, K. Yasumoto, and C. H. Liang, "Two-dimensional scattering of a Gaussian beam by a periodic array of circular cylinders," *IEEE Transactions on Geoscience and Remote Sensing*, Vol. 43, No. 2, 280–285, 2005.
9. Wang, X. D., Y. B. Gan, and L. W. Li, "Electromagnetic scattering by partially buried PEC cylinder at the dielectric rough surface interface: TM case," *IEEE Antennas and Wireless Propagation Letters*, Vol. 2, 319–322, 2003.
10. Yang, J., L. W. Li, and C. H. Liang, "Two-dimensional scattering by a periodic array of gyrotropic cylinders embedded in a dielectric slab," *IEEE Antennas and Wireless Propagation Letters*, Vol. 2, No. 1, 18–21, 2003.
11. Yin, W. Y., L. W. Li, and M. S. Leong, "Scattering from multiple bianisotropic cylinders and their modeling of cylindrical objects of arbitrary cross-section," *Progress In Electromagnetics Research*, PIER 27, 159–184, 2000.
12. Truman, C. W., S. J. Kubina, S. R. Mishra, and C. Larose, "Radar cross-section of a generic aircraft at HF frequencies," *Canadian J. Elect. Comp. Eng*, Vol. 18, No. 2, 59–62, 1993.
13. Sevgi, L. and S. Paker,"FDTD based RCS calculations and antenna simulation," *AEU, International J. of Electronics*, Vol. 52, No. 2, 65–75, 1986.
14. Gurel, L., H. Bagei, J. C. Castelli, A. Cheraly, and F. Tardivel, "Validation through comparison, measurement and calculation of bistatic RCS of a stealth target," *Radio Science*, Vol. 38, No. 3, 1046–1057, 2003.
15. Sevgi, L., *Complex Electromagnetic Problems and Numerical Simulation Approaches,* IEEE & John Wiley Press, 2003.
16. Tang, C. C. H., "Backscattering from dielectrically coated infinite cylindrical obstacles," *J. Appl. Phys.*, Vol. 28, 628–633, 1957.

17. Hill, S. C. and J. M. Jarem, "Scattering of multilayer concentric elliptical cylinders excited by single mode source," *Progress In Electromagnetics Research*, PIER 55, 209–226, 2005.
18. Anastassiu, H. T., "Error estimation of the method of auxiliary sources (MAS) for scattering from an impedance circular cylinder," *Progress In Electromagnetics Research*, PIER 52, 109–128, 2005.
19. Vinoy, K. J. and R. M. Jha, *Radar Absorbing Materials: From Theory to Design and Characterizaton,* Kluwer Academic Publishers, Masschusetts, 1996.
20. Ramprecht, J. and D. Sjeberg, "Biased magnetic materials in RAM applications," *Progress In Electromagnetics Research*, PIER 75, 85–117, 2007.
21. Mittra, R. and O. Ramahi, "Absorbing boundary conditions for the direct solution of partial differential equations arising in electromagnetic scattering problems," *Progress In Electromagnetics Research*, PIER 02, 133–173, 1990.
22. Jaggard, D. L. and N. Engheta," Chiro-shield: a Salisbury/Dallenbach shield alternative," *Electron. Lett.*, Vol. 26, No. 17, 1332–1334, 1990.
23. Ishimaru, A., *Electromagnetic Wave Propagation, Radiation, and Scattering*, Prentice-Hall, Englewood Cliffs, 1991.
24. Li, C. and Z. Shen, "Electromagnetic scattering by a conducting cylinder coated with metamaterials," *Progress In Electromagnetics Research*, PIER 42, 91–105, 2003.
25. Richmond, J. R., "Scattering by a dielectric cylinder of arbitrary cross-section shape," *IEEE Trans. Antennas and Propag.*, Vol. 13, 334–341, 1965.
26. Yao, H. Y., L. W. Li, C. W. Qiu, Q. Wu, and Z. N. Chen, "Scattering properties of electromagnetic wave in a multilayerd cylinder filled with double negative and positive materials," *Radio Science*, Vol. 42, 2007.
27. Tang, C. C. H., "Backscattering from dielectrically coated infinite cylindrical obstacles," Ph.D. Thesis, Havard University, 1956.
28. Oraizi, H., "Application of the method of least squares to electromagnetic engineering problems," *IEEE Antenna and Propagation Magazine*, Vol. 48, No. 1, 50–75, 2006.
29. Tah-Hsiung, C., "Polarization effects on microwave imaging of dielectric cylinder," *IEEE Transactions on Microwave Theory and Techniques*, Vol. 36, No. 9, 1366–1369, 1988.